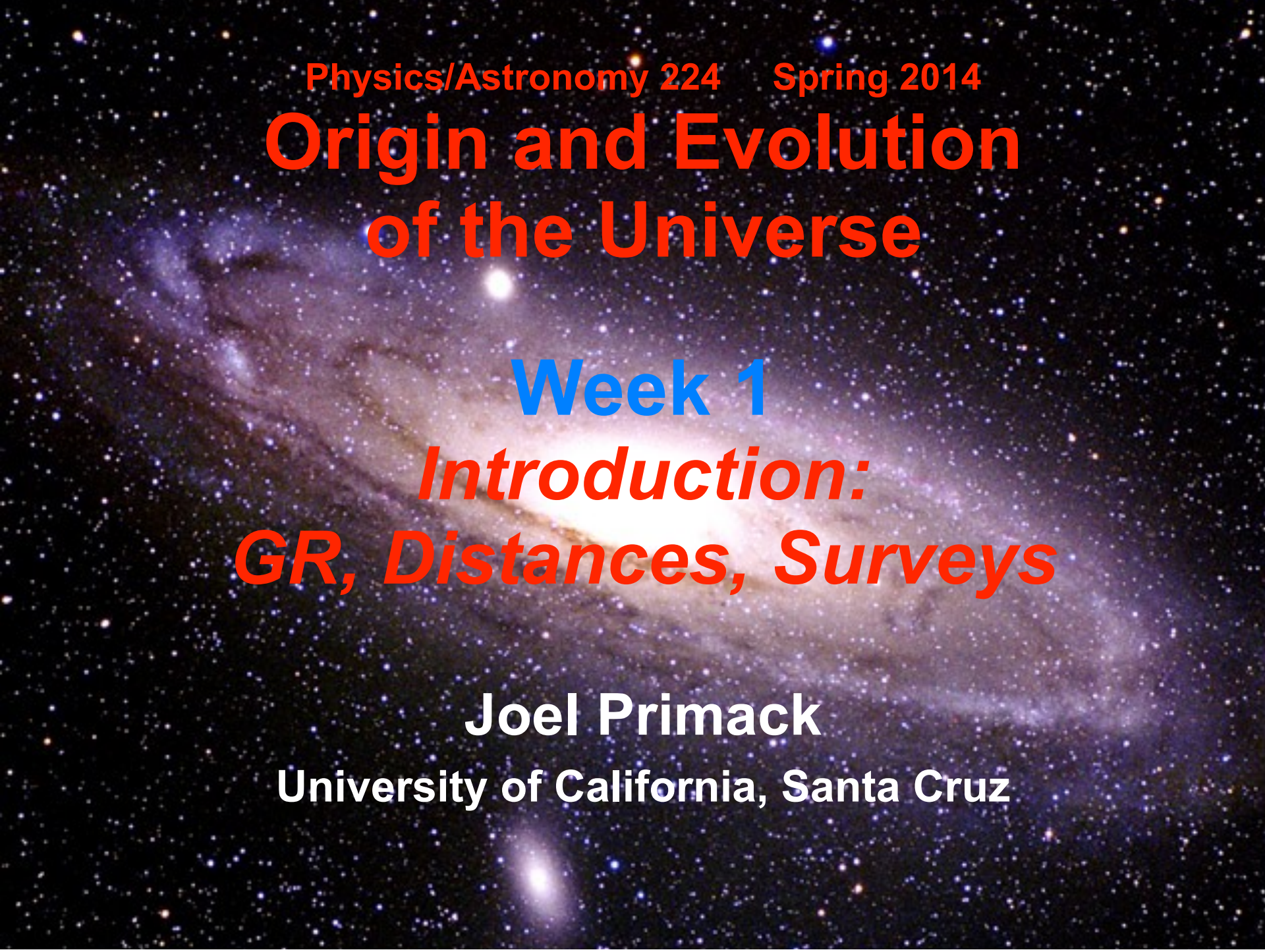
Physics/Astronomy 224 Spring 2014
Origin and Evolution of the Universe
Week 1
Introduction:
GR, Distances, Surveys
Joel Primack
University of California, Santa Cruz

Physics 224 **Origin and Evolution of the Universe** Spring 2014

Tuesday-Thursday 12:00-1:45 pm in ISB 231

Instructor: Joel Primack – office hours: Thurs 2:00-3:00 pm or by appointment
Office: ISB 318, phone: 459-2580, email: joel@ucsc.edu

Catalog Description: Introduction to the particle physics and cosmology of the very early universe: relativistic cosmology, initial conditions, inflation and grand unified theories, baryogenesis, nucleosynthesis, gravitational collapse, hypotheses regarding the dark matter and consequences for formation of galaxies and large scale structure. Offered in alternate academic years.

Students will be expected to do several homework assignments, and also a term project to be presented orally at the end of the course. Lectures and homework will be posted at physics.ucsc.edu/~joel/Phys224 . We will not follow any one textbook, but I particularly recommend Abraham Loeb, *How Did the First Stars and Galaxies Form?* (Princeton University Press, 2010) and Scott Dodelson, *Modern Cosmology* (Academic Press, 2003), which I have asked Bay Tree Bookstore to order.

Introduction

Modern cosmology – the study of the universe as a whole – is undergoing a scientific revolution. We can see back in time to the cosmic dark ages before galaxies formed and read the history of the early universe in the ripples of heat radiation still arriving from the Big Bang. We now know that everything that we can see makes up only about ½% of the cosmic density, and that most of the universe is made of invisible stuff called "dark matter" and "dark energy." The ΛCDM Dark Energy + Cold Dark Matter ("Double Dark") theory based on this appears to be able to account for all the large scale features of the observable universe, including the heat radiation and the large scale distribution of galaxies, although there are possible problems understanding some details of the structure of galaxies.

Modern cosmology is developing humanity's first story of the origin and nature of the universe that might actually be true.

Modern Cosmology

A series of major discoveries has laid a lasting foundation for cosmology. Einstein's general relativity (1916) provided the conceptual foundation for the modern picture. Then Hubble discovered that "spiral nebulae" are large galaxies like our own Milky Way (1924), and that distant galaxies are receding from the Milky Way with a speed proportional to their distance (1929), which means that we live in an expanding universe. The discovery of the cosmic background radiation (1965) showed that the universe began in a very dense, hot, and homogeneous state: the Big Bang. This was confirmed by the discovery that the cosmic background radiation has exactly the same spectrum as heat radiation (1989), and the measured abundances of the light elements agree with the predictions of Big Bang theory if the abundance of ordinary matter is about 4% of critical density. Most of the matter in the universe is invisible particles which move very sluggishly in the early universe ("Cold Dark Matter"). Most of the energy density is mysterious dark energy.

Experimental and Historical Sciences

both make predictions about new knowledge, whether from experiments or from the past

Historical Explanation Is Always Inferential

Our age cannot look back to earlier things
Except where reasoning reveals their traces Lucretius

Patterns of Explanation Are the Same in the Historical Sciences as in the Experimental Sciences

Specific conditions + General laws ⇒ Particular event

In history as anywhere else in empirical science, the explanation of a phenomenon consists in subsuming it under general empirical laws; and the criterion of its soundness is … exclusively whether it rests on empirically well confirmed assumptions concerning initial conditions and general laws.

C.G. Hempel, *Aspects of Scientific Explanation* (1965), p. 240.

Successful Predictions of the Big Bang

First Prediction	First Confirmation
Expansion of the Universe	
Friedmann 1922, Lemaitre 1927 based on Einstein 1916	Hubble 1929
Cosmic Background Radiation	
Existence of CBR Gamow, Alpher, Hermann 1948	Penzias & Wilson 1965
CBR Thermal Spectrum Peebles 1966	COBE 1989
CBR Fluctuation Amplitude Cold Dark Matter theory 1984	COBE 1992
CBR Acoustic Peak	BOOMERANG 2000 MAXIMA 2000
Light Element Abundances	
Peebles 1966, Wagoner 1967	D/H Tytler et al. 1997

Three Pillars of the Big Bang

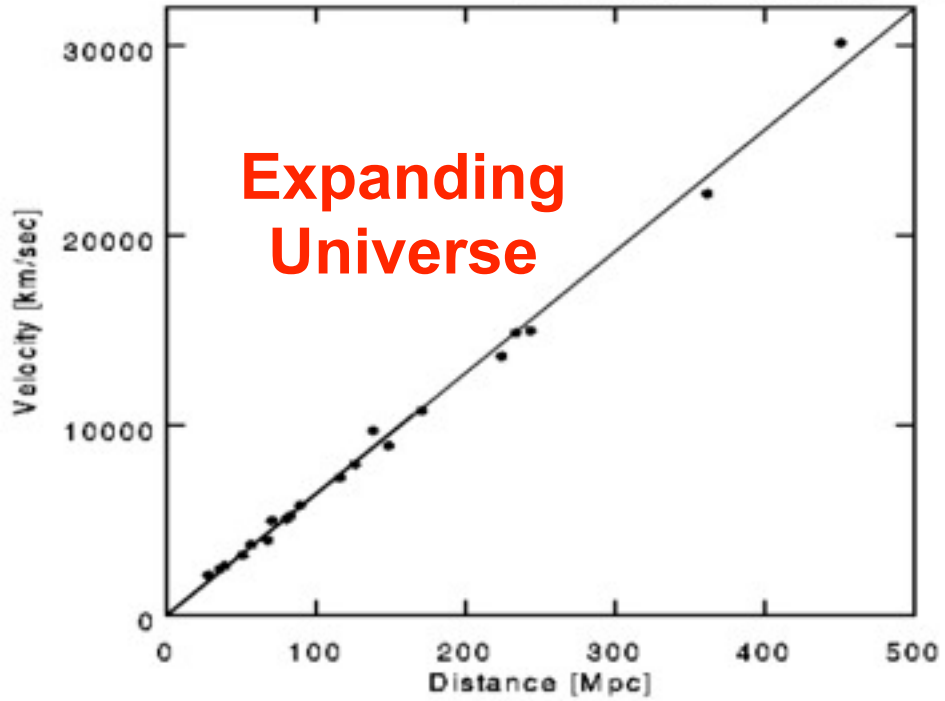

A modern illustration of Hubble's Law, displaying the increase of recession speed of galaxies growing in direct proportion to their distance.

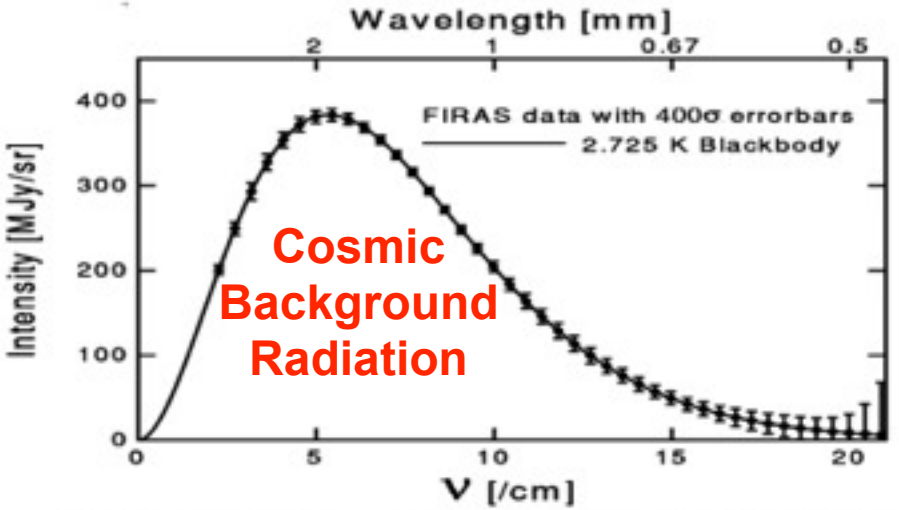

The variation of the intensity of the microwave background radiation with its frequency, as observed by the COBE satellite from above the Earth's atmosphere. The observations (boxes) display a perfect fit with the (solid) curve expected from pure heat radiation with a temperature of 2.73°K.

Big Bang Nucleosynthesis

The detailed production of the lightest elements out of protons and neutrons during the first three minutes of the universe's history. The nuclear reactions occur rapidly when the temperature falls below a billion degrees Kelvin. Subsequently, the reactions are shut down, because of the rapidly falling temperature and density of matter in the expanding universe.

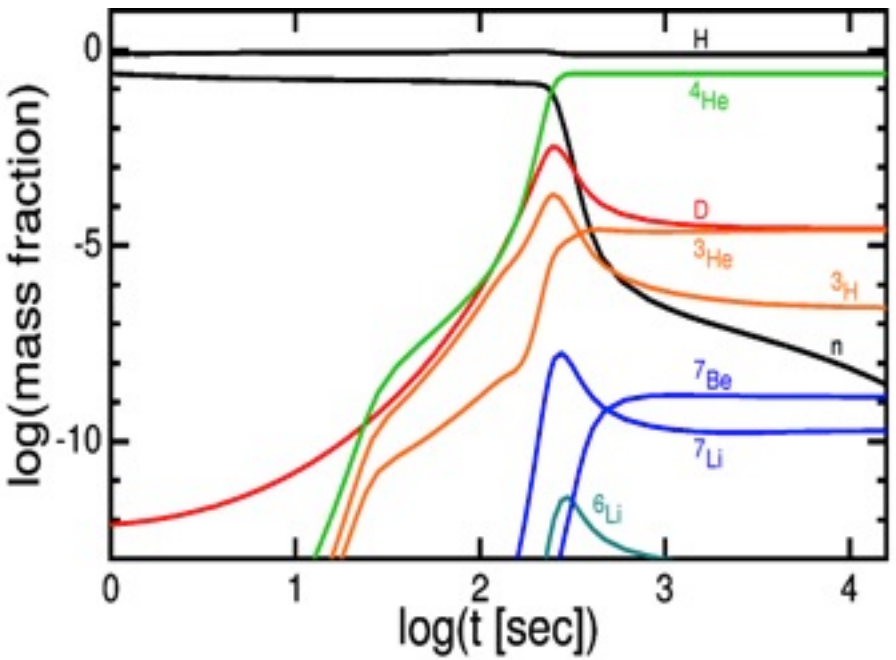

Caution: ^{7}Li may now be discordant

Mon. Not. R. astr. Soc. (1991) 251, 128-136

Dynamical effects of the cosmological constant

Ofer Lahav,[1] Per B. Lilje,[2] Joel R. Primack[3] and Martin J. Rees[1]

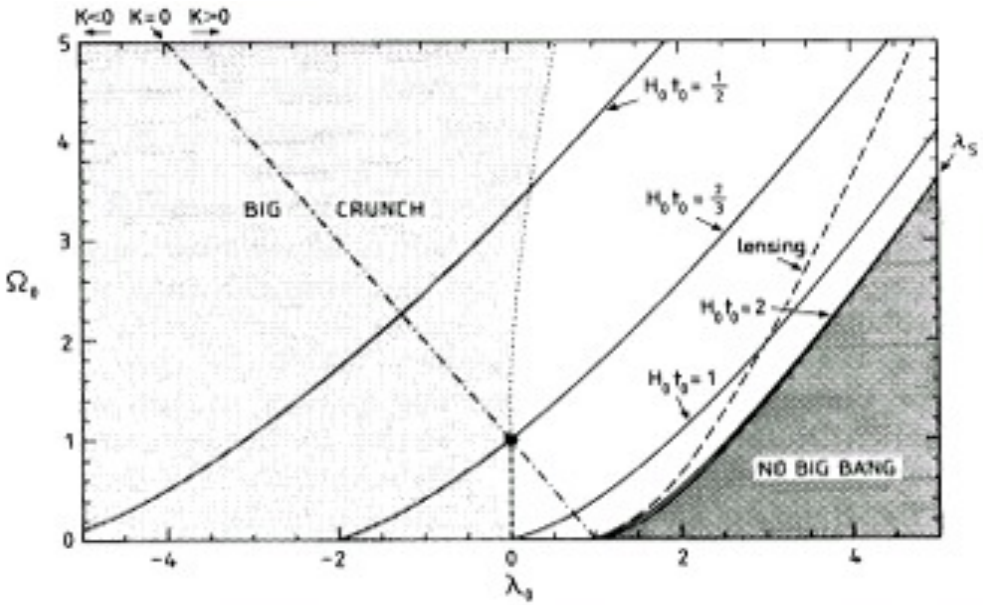

Figure 1. The phase-space of the density parameter Ω_0 and the cosmological constant $\lambda_0 \equiv \Lambda/(3H_0^2)$ with various fundamental constraints. The dashed-dotted line indicates an inflationary (i.e. flat) universe. Note that some open models will have a Big Crunch, while some closed models will expand forever. The solid lines show 4 values for the age of the universe H_0t_0, and the dashed line is the constraint of Gott *et al.* (1989) from a normally lensed quasar at $z = 3.27$. The boundary (λ_s) of the shaded 'No Big Bang' region corresponds to a coasting phase in the past, while the boundary of the 'Big Crunch' (for $\Omega_0 > 1$) region corresponds to a coasting phase in the future. We see that the permitted range in the $(\lambda_0 - \Omega_0)$ phase-space is fairly small, but allows values different from the popular point $(\Omega_0 = 1, \lambda_0 = 0)$.

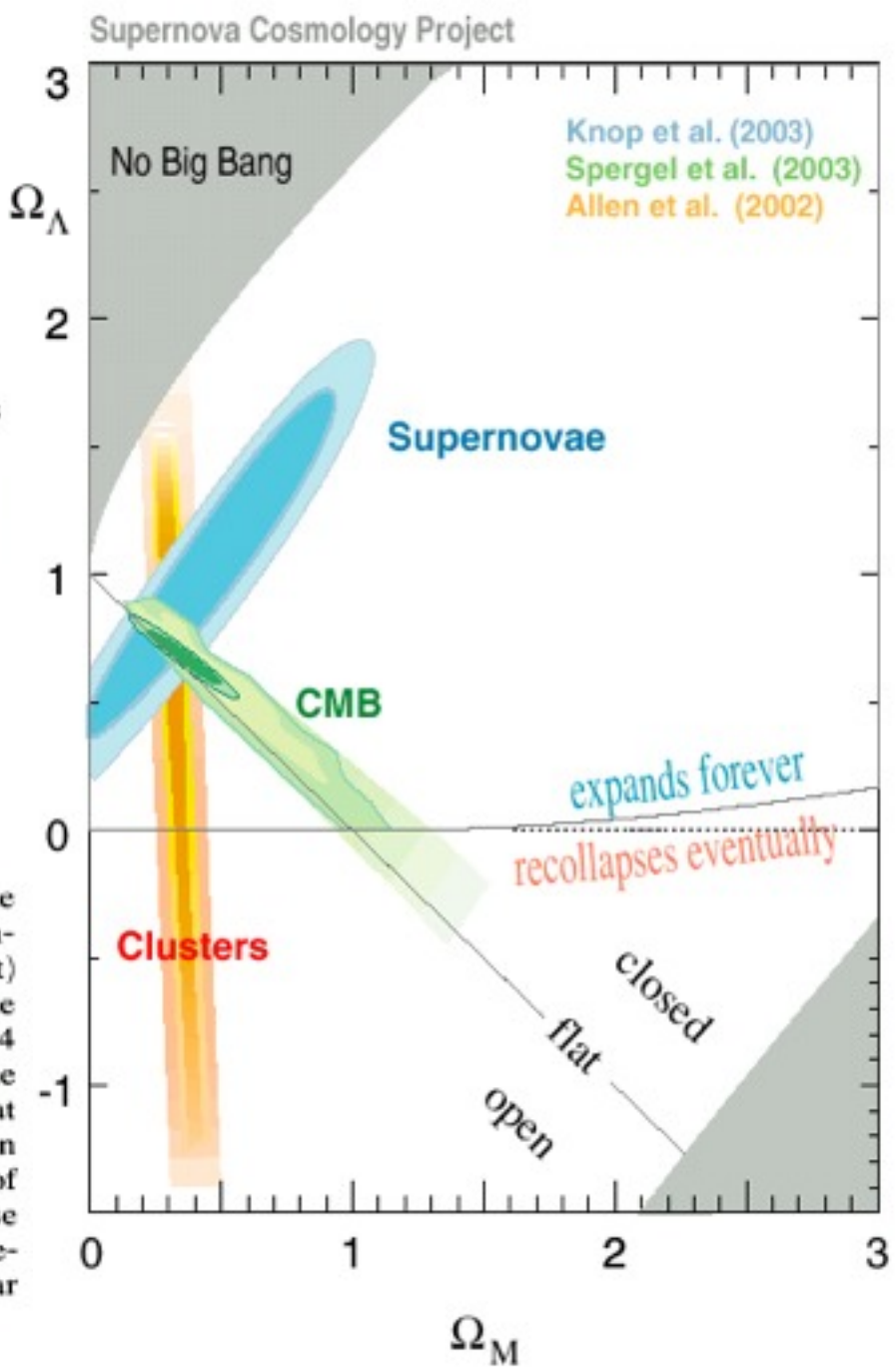

Special Relativity is based on two postulates

- All the laws of physics are the same in all inertial reference frames.
- The speed of light is the same for all inertial observers, regardless of their velocity or that of the source of the light.

Einstein realized that Newton's theory of gravity, with instantaneous action at a distance, could not be compatible with special relativity -- which undermined the concept of simultaneous events at a distance. It took 10 years for Einstein to get the right idea for the right theory, but then in only two months in late 1915 he worked out the theory and its main initial predictions: the precession of the orbit of Mercury, bending of light by the sun, and the slowing of clocks by gravity.

General Relativity is also based on two postulates

- Equivalence Principle: All the effects of gravity on small scales are the same as those of acceleration. (Thus gravity is eliminated in local inertial = free fall frames.)
- Einstein's Field Equations: $G_{\mu\nu} = -(8\pi G/c^4) T_{\mu\nu}$ where $G_{\mu\nu} = R_{\mu\nu} - \frac{1}{2} R\, g_{\mu\nu}$ describes the curvature of space-time at each point and $T_{\mu\nu}$ describes the mass-energy, momentum, and stress density at the same point.

General Relativity

CURVED SPACE TELLS MATTER HOW TO MOVE

$$\frac{du^\mu}{ds} + \Gamma^\mu{}_{\alpha\beta}\, u^\alpha u^\beta = 0$$

MATTER TELLS SPACE HOW TO CURVE

Einstein Field Equations

$$G^{\mu\nu} \equiv R^{\mu\nu} - \tfrac{1}{2}Rg^{\mu\nu} = -8\pi G T^{\mu\nu} - \Lambda g^{\mu\nu}$$

Here u^α is the velocity 4-vector of a particle. The Ricci curvature tensor $R_{\mu\nu} \equiv R_{\lambda\mu\sigma\nu}g^{\lambda\sigma}$, the Riemann curvature tensor $R^\lambda{}_{\mu\sigma\nu}$, and the affine connection $\Gamma^\mu{}_{\alpha\beta}$ can be calculated from the metric tensor $g_{\lambda\sigma}$. If the metric is just that of flat space, then $\Gamma^\mu{}_{\alpha\beta} = 0$ and the first equation above just says that the particle is unaccelerated -- i.e., it satisfies the law of inertia (Newton's 1st law).

General Relativity

CURVED SPACE TELLS MATTER HOW TO MOVE

$$\frac{du^\mu}{ds} + \Gamma^\mu{}_{\alpha\beta}\, u^\alpha u^\beta = 0$$

MATTER TELLS SPACE HOW TO CURVE

Einstein Field Equations

$$G^{\mu\nu} \equiv R^{\mu\nu} - \tfrac{1}{2}Rg^{\mu\nu} = -8\pi G T^{\mu\nu} - \Lambda g^{\mu\nu}$$

Curved spacetime is not just an arena within which things happen, spacetime is dynamic. Curvature can even cause horizons, beyond which information cannot be sent.

There are event horizons around black holes and we are also surrounded by both particle and event horizons.

General Relativity and Cosmology

CURVED SPACE TELLS MATTER HOW TO MOVE

$$\frac{du^\mu}{ds} + \Gamma^\mu{}_{\alpha\beta}\, u^\alpha u^\beta = 0$$

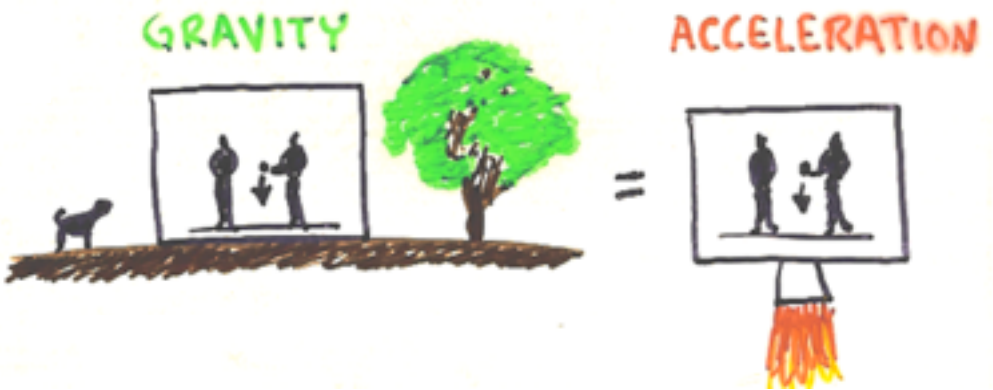

MATTER TELLS SPACE HOW TO CURVE

Einstein Field Equations

$$G^{\mu\nu} \equiv R^{\mu\nu} - \tfrac{1}{2}Rg^{\mu\nu} = -8\pi G T^{\mu\nu} - \Lambda g^{\mu\nu}$$

Einstein's Cosmological Principle: on large scales, space is uniform and isotropic.

COBE-Copernicus Theorem: If all observers observe a nearly-isotropic Cosmic Background Radiation (CBR), then the universe is locally nearly homogeneous and isotropic – i.e., is approximately described by the Friedmann-Robertson-Walker metric:

$$ds^2 = dt^2 - a^2(t)\,[dr^2\,(1 - kr^2)^{-1} + r^2\, d\Omega^2]$$

with curvature constant k = –1, 0, or +1. Substituting this metric into the Einstein equations above, we get the Friedmann equations.

Friedmann-Robertson-Walker Metric

(homogeneous, isotropic universe)

$$\text{FRW E}(00) \quad \frac{\dot{a}^2}{a^2} = \frac{8\pi}{3}G\rho - \frac{k}{a^2} + \frac{\Lambda}{3}$$ ← Friedmann equation

$$\text{FRW E}(ii) \quad \frac{2\ddot{a}}{a} + \frac{\dot{a}^2}{a^2} = -8\pi G p - \frac{k}{a^2} + \Lambda$$

$$H_0 \equiv 100h\,\mathrm{km\,s^{-1}Mpc^{-2}} \equiv 70h_{70}\,\mathrm{km\,s^{-1}Mpc^{-2}}$$

$$\frac{E(00)}{H_0^2} \Rightarrow 1 = \Omega_0 - \frac{k}{H_0^2} + \Omega_\Lambda \text{ with } H \equiv \frac{\dot{a}}{a},\ a_0 \equiv 1,\ \Omega_0 \equiv \frac{\rho_0}{\rho_c}, \Omega_\Lambda \equiv \frac{\Lambda}{3H_0^2},$$

$$\rho_{c,0} \equiv \frac{3H_0^2}{8\pi G} = 1.36 \times 10^{11} h_{70}^2 M_\odot \mathrm{Mpc}^{-3}$$

$$E(ii) - E(00) \Rightarrow \frac{2\ddot{a}}{a} = -\frac{8\pi}{3}G\rho - 8\pi G p + \frac{2}{3}\Lambda$$

$$\text{Divide by } 2E(00) \Rightarrow \quad q_0 \equiv -\left(\frac{\ddot{a}}{a}\frac{a^2}{\dot{a}^2}\right)_0 = \frac{\Omega_0}{2} - \Omega_\Lambda$$ ← deceleration parameter

$$E(00) \Rightarrow t_0 = \int_0^1 \frac{da}{a}\left[\frac{8\pi}{3}G\rho - \frac{k}{a^2} + \frac{\Lambda}{3}\right]^{-\frac{1}{2}} = H_0^{-1}\int_0^1 \frac{da}{a}\left[\frac{\Omega_0}{a^3} - \frac{k}{H_0^2 a^2} + \Omega_\Lambda\right]^{-\frac{1}{2}}$$

$$t_0 = H_0^{-1} f(\Omega_0, \Omega_\Lambda) \qquad H_0^{-1} = 9.78h^{-1}\mathrm{Gyr}$$

$$f(1,0) = \tfrac{2}{3}$$
$$f(0,0) = 1$$
$$f(0,1) = \infty$$

age of the universe

$$\frac{E(00)}{H_0^2} \Rightarrow 1 = \Omega_0 - \frac{k}{H_0^2} + \Omega_\Lambda \text{ with } H \equiv \frac{\dot{a}}{a},\ a_0 \equiv 1,\ \Omega_0 \equiv \frac{\rho_0}{\rho_c}, \Omega_\Lambda \equiv \frac{\Lambda}{3H_0^2},$$

$$\rho_{c,0} \equiv \frac{3H_0^2}{8\pi G} = 1.36 \times 10^{11} h_{70}^2 M_\odot \mathrm{Mpc}^{-3}$$

$$E(ii) - E(00) \Rightarrow \frac{2\ddot{a}}{a} = -\frac{8\pi}{3} G\rho - 8\pi G p + \frac{2}{3}\Lambda$$

$$\text{Divide by } 2E(00) \Rightarrow \quad q_0 \equiv -\left(\frac{\ddot{a}}{a}\frac{a^2}{\dot{a}^2}\right)_0 = \frac{\Omega_0}{2} - \Omega_\Lambda$$

$$E(00) \Rightarrow t_0 = \int_0^1 \frac{da}{a}\left[\frac{8\pi}{3}G\rho - \frac{k}{a^2} + \frac{\Lambda}{3}\right]^{-\frac{1}{2}} = H_0^{-1}\int_0^1 \frac{da}{a}\left[\frac{\Omega_0}{a^3} - \frac{k}{H_0^2 a^2} + \Omega_\Lambda\right]^{-\frac{1}{2}}$$

$$t_0 = H_0^{-1} f(\Omega_0, \Omega_\Lambda) \qquad H_0^{-1} = 9.78 h^{-1}\mathrm{Gyr} \qquad f(1,0) = \tfrac{2}{3}$$

$$f(0,0) = 1$$

$$f(0,1) = \infty$$

age of the universe

$$[E(00)a^3]' \text{ vs. } E(ii) \Rightarrow \quad \frac{\partial}{\partial a}(\rho a^3) = -3pa^2 \text{ (“continuity”)}$$

Given eq. of state $p = p(\rho)$, integrate to determine $\rho(a)$,
integrate $E(00)$ to determine $a(t)$

Examples: $p = 0 \Rightarrow \rho = \rho_0 a^{-3}$ (assumed above in q_0, t_0 eqs.)

$p = \frac{\rho}{3},\ k = 0 \Rightarrow \rho \propto a^{-4}$

Measuring Distances in the Universe

Primary Distance Indicators

Trigonometric parallax

α Centauri 1.35 pc - first measured by Thomas Henderson 1832

61 Cygni 3.48 pc - by Friedrich Wilhelm Bessel in 1838

Only a few stars to < 30 pc, until the Hipparcos satellite 1997 measured distances of 118,000 stars to about 100 pc, about 20,000 stars to <10%.

Proper motions

Moving cluster method

Mainly for the Hyades, at about 100 pc. Now supplanted by Hipparcos.

Distance to Cepheid ζ Geminorum = 336 ± 44 pc

Using Doppler to measure change of diameter, and interferometry to measure change of angular diameter.

Similar methods for Type II SN, for stars in orbit about the Sagittarius A* SMBH (gives distance 8.0 ± 0.4 kpc to Galactic Center), for radio maser in NGC 4258 (7.2 ± 0.5 Mpc), etc.

Apparent Luminosity of various types of stars

$L = 10^{-2M/5}\ 3.02\times10^{35}$ erg sec^{-1} where $M_{vis} = +4.82$ for the sun

Apparent luminosity $\ell = L\,(4\pi d^2)^{-1}$ for nearby objects,
related to apparent magnitude m by $\ell = 10^{-2m/5}\ (2.52\times10^{-5}$ erg cm^{-2} s$^{-1})$

Distance modulus m - M related to distance by $d = 10^{1\ +\ (m\ -\ M)/5}$ pc

Main sequence stars were calibrated by Hipparchos distances
and the Hubble Space Telescope Fine Guidance Sensor
Red clump (He burning) **stars**.
RR Lyrae Stars - variables with periods 0.2 - 0.8 days
Eclipsing binaries - v from Doppler, ellipticity from v(t), radius of primary from duration of eclipse, T from spectrum, gives $L = \sigma T^4\ \pi R^2$
Cepheid variables - bright variable stars with periods 2 - 45 days

Henrietta Swan Leavitt in 1912 discovered the Cepheid period-luminosity relation in the SMC, now derived mainly from the LMC. This was the basis for Hubble's 1923 finding that M31 is far outside the Milky Way. Best value today for the LMC distance modulus m - M = 18.50 (see Weinberg, *Cosmology*, p. 25), or $d_{LMC} = 50.1$ kpc.

Hertzsprung-Russell Diagram

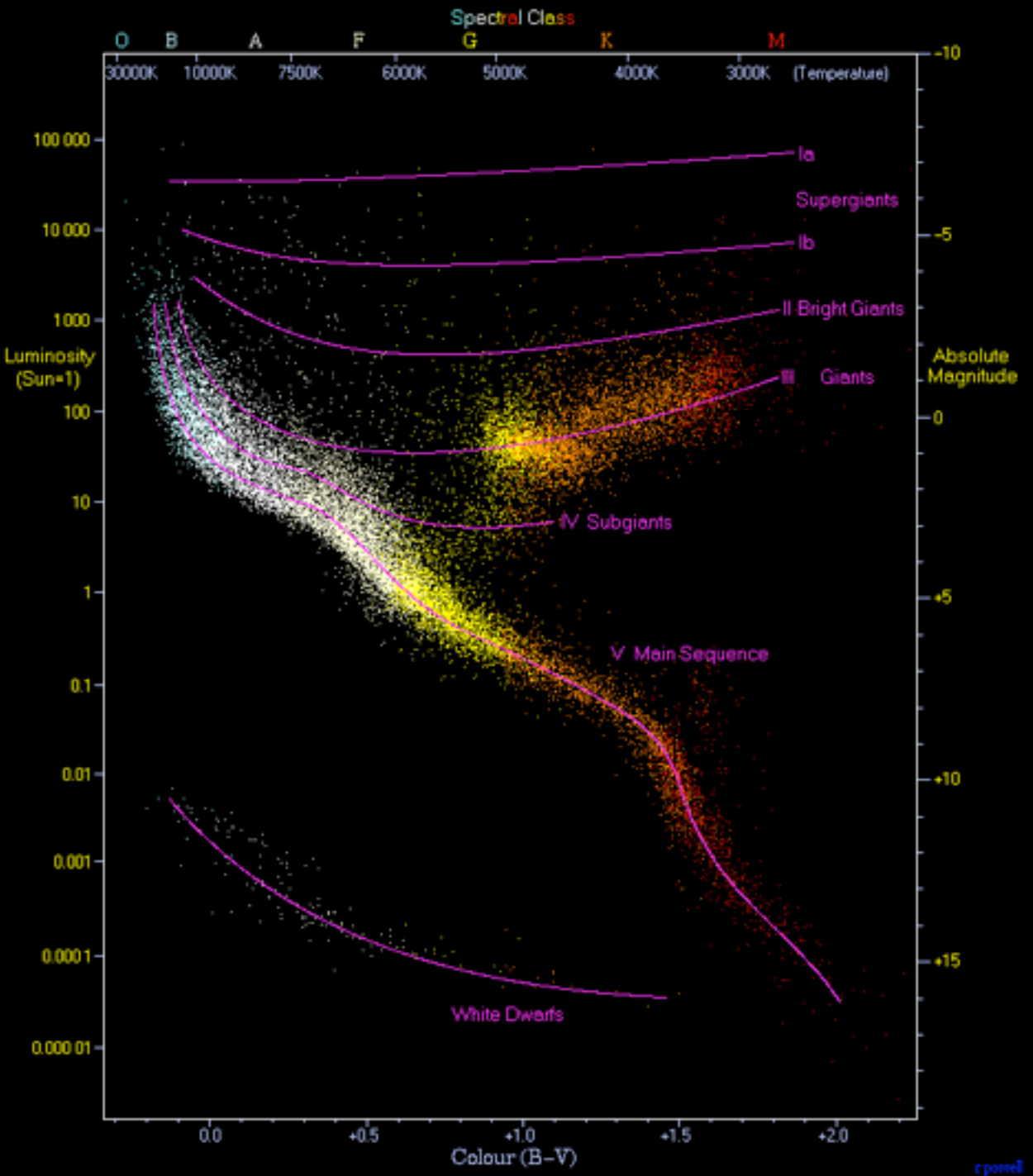

Hertzsprung-Russell Diagram

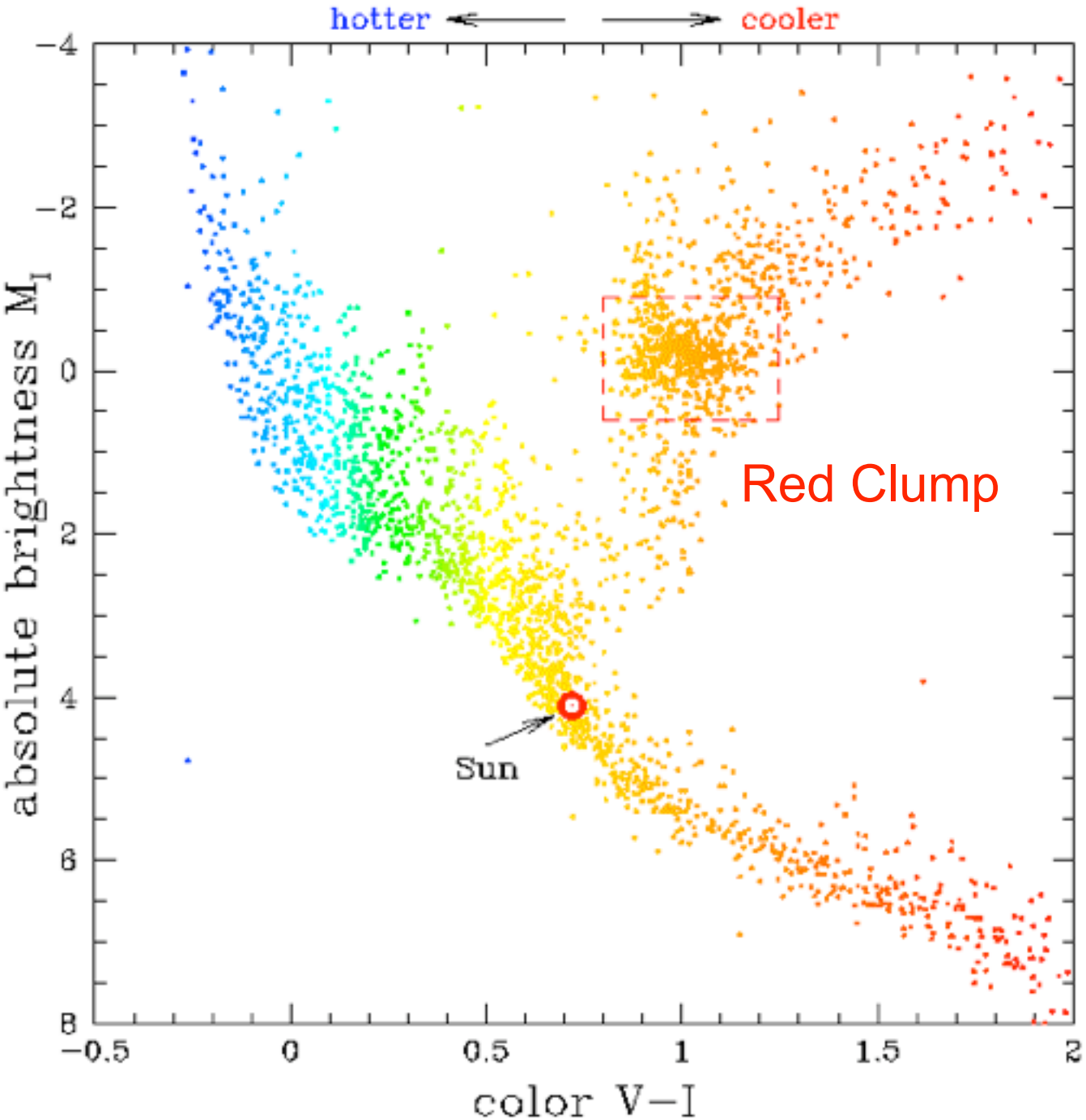

Secondary Distance Indicators

Tully-Fisher relation: $L \sim V_{rot}^4$

Faber-Jackson relation: $L \sim \sigma^4$

Fundamental plane

Type Ia supernovae

Surface brightness fluctuations

Extragalactic water masers

Planck errors are small and Planck's value for H_0 is smaller than from WMAP9 and Riess+2011

Recent Hubble Parameter Determinations

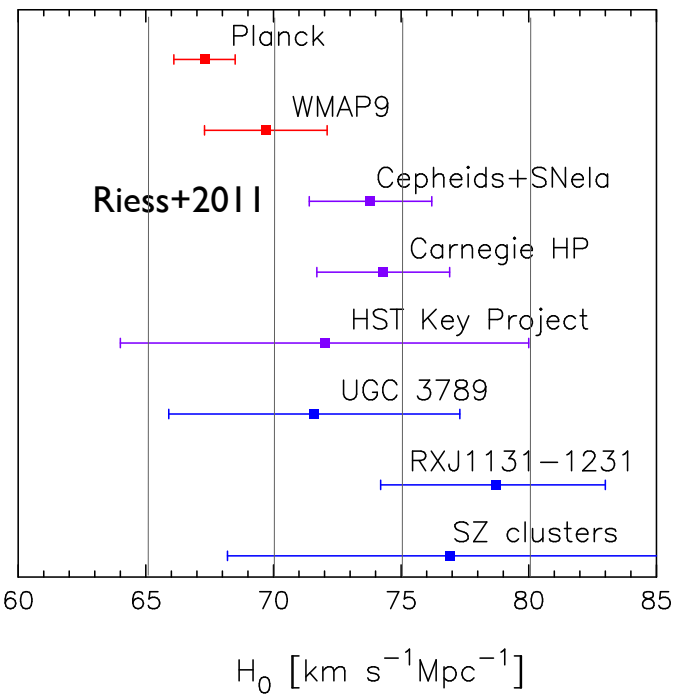

Extragalactic water masers

A geometric distance to the galaxy NGC4258 from orbital motions in a nuclear gas disk

J. R. Herrnstein et al. 1999, Nature, 400, 539. Dist to NGC4258 = 7.2±0.3 Mpc.

The distance is found by measuring the time-varying Doppler shift and proper motion around the central black hole. The Doppler shift is maximum when an object is moving along the l.o.s. and the proper motion is maximum when the object is moving perpendicular to the l.o.s.

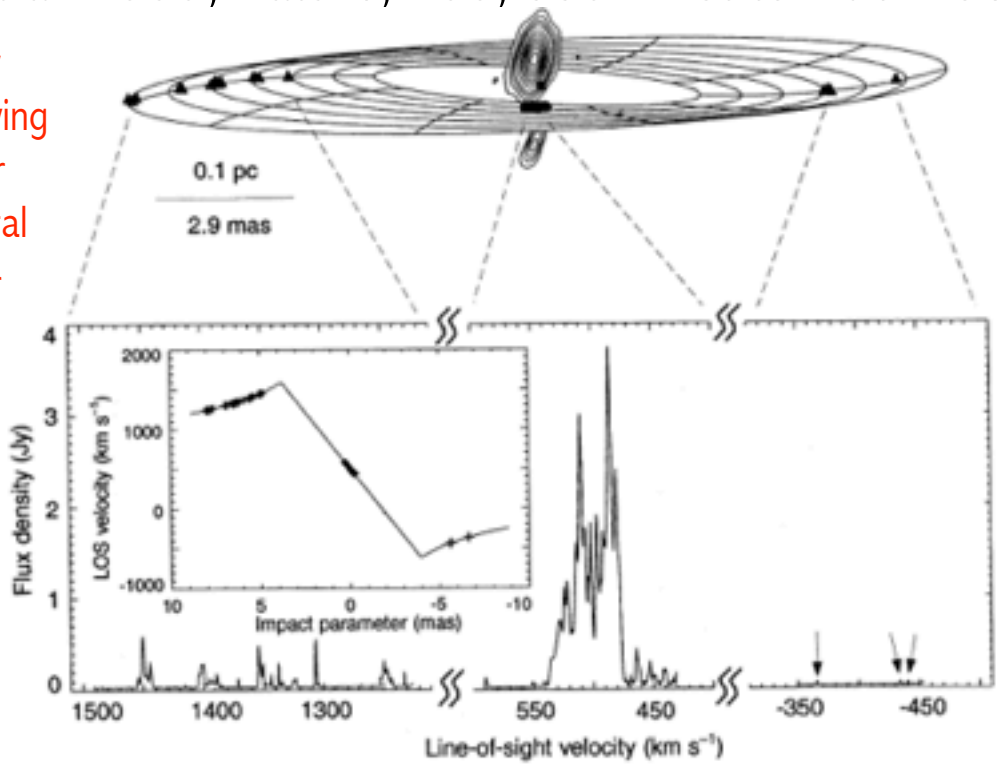

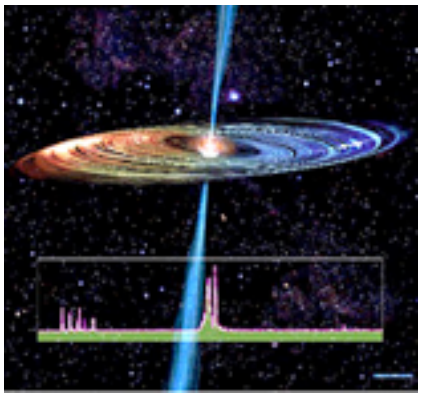

Artist's Conception

$M_{BH} = 3.9 \pm 0.1\ M_{sun}$

Figure 1 The NGC4258 water maser. The upper panel shows the best-fitting warped-disk model superposed on actual maser positions as measured by the VLBA of the NRAO, with top as North. The filled square marks the centre of the disk, as determined from a global disk-fitting analysis[8]. The filled triangles show the positions of the high-velocity masers, so called because they occur at frequencies corresponding to Doppler shifts of ~±1,000 km s^{-1} with respect to the galaxy systemic velocity of ~470 km s^{-1}. This is apparent in the VLBA total power spectrum (lower panel). The inset shows line-of-sight (LOS) velocity versus impact parameter for the best-fitting keplerian disk, with the maser data superposed. The high-velocity masers trace a keplerian curve to better than 1%. Monitoring of these features indicates that they drift by less than ~1 km s^{-1} yr^{-1} (refs 14–16) and requires that they lie within 5–10° of the midline, the intersection of the disk with the plane of the sky. The LOS velocities of the systemic masers are centred about the systemic velocity of the galaxy. The positions (filled circles in upper panel) and LOS velocities of these masers imply that they subtend ~8° of disk azimuth centred about the LOS to the central mass, and the observed acceleration (8–10 km s^{-1} yr^{-1}) of these features[14,15] unambiguously places them along the near edge of the disk. The approximately linear relationship between systemic maser impact parameter and LOS velocity demonstrates that the disk is very thin[17] (aspect ratio ≤ 0.2%) and that these masers are confined to a narrow annulus in the disk. The magnitude of the velocity gradient (Ω_s) implies a mean systemic radius, (r_s), of 3.9 mas which, together with the positions of the high-velocity masers, constrains the disk inclination, i_s, to be ~82 ± 1° (90° for edge-on). Finally, VLBA continuum images[7,13] are included as contours in the upper panel. The 22-GHz radio emission traces a sub-parsec-scale jet elongated along the rotation axis of the disk and well-aligned with a luminous, kiloparsec-scale jet[18].

Extragalactic water masers

A geometric distance to the galaxy NGC4258 from orbital motions in a nuclear gas disk

J. R. Herrnstein et al. 1999, Nature, 400, 539. Dist to NGC4258 = 7.2±0.3 Mpc.

we conclude that $\langle \dot{v}_{\rm LOS} \rangle = 9.3 \pm 0.3\,{\rm km\,s^{-1}\,yr^{-1}}$ and $\langle \dot{\theta}_x \rangle = 31.5 \pm 1\,\mu{\rm as\,yr^{-1}}$, where these (and all subsequent) uncertainties are 1σ values.

To convert the maser proper motions and accelerations into a geometric distance, we express $\langle \dot{\theta}_x \rangle$ and $\langle \dot{v}_{\rm LOS} \rangle$ in terms of the distance and four disk parameters:

$$\langle \dot{\theta}_x \rangle = 31.5 \left[\frac{D_6}{7.2}\right]^{-1} \left[\frac{\Omega_s}{282}\right]^{1/3} \left[\frac{M_{7.2}}{3.9}\right]^{1/3} \left[\frac{\sin i_s}{\sin 82.3^\circ}\right]^{-1} \left[\frac{\cos \alpha_s}{\cos 80^\circ}\right] \mu{\rm as\,yr^{-1}} \quad (1)$$

and

$$\langle \dot{v}_{\rm LOS} \rangle = 9.2 \left[\frac{D_6}{7.2}\right]^{-1} \left[\frac{\Omega_s}{282}\right]^{4/3} \left[\frac{M_{7.2}}{3.9}\right]^{1/3} \left[\frac{\sin i_s}{\sin 82.3^\circ}\right]^{-1} {\rm km\,s^{-1}\,yr^{-1}} \quad (2)$$

Here D_6 is the distance in Mpc, α_s is the disk position angle (East of North) at $\langle r_s \rangle$, and $M_{7.2}$ is $M/D \sin^2 i_s$ as derived from the high-velocity rotation curve and evaluated at $D = 7.2$ Mpc and $i_s = 82.3^\circ$ (in units of $10^7\,M_\odot$). $\Omega_s \equiv (GM_{7.2}/\langle r_s \rangle^3)^{1/2}$ is the projected disk angular velocity at $\langle r_s \rangle$

Extragalactic water masers

A geometric distance to the galaxy NGC4258 from orbital motions in a nuclear gas disk
J. R. Herrnstein et al. 1999, Nature, 400, 539. Dist to NGC4258 = 7.2±0.3 Mpc.

The Astrophysical Journal, 775:13 (10pp), 2013 September 1

TOWARD A NEW GEOMETRIC DISTANCE TO THE ACTIVE GALAXY NGC 4258. III. FINAL RESULTS AND THE HUBBLE CONSTANT

E. M. L. Humphreys[1,2], M. J. Reid[2], J. M. Moran[2], L. J. Greenhill[2], and A. L. Argon[2]
[1] European Southern Observatory, Karl-Schwarzschild-Str. 2, D-85748 Garching bei München, Germany; ehumphre@eso.org
[2] Harvard-Smithsonian Center for Astrophysics, 60 Garden Street, Cambridge, MA 02138, USA
Received 2012 December 4; accepted 2013 July 22; published 2013 August 29

ABSTRACT

We report a new geometric maser distance estimate to the active galaxy NGC 4258. The data for the new model are maser line-of-sight (LOS) velocities and sky positions from 18 epochs of very long baseline interferometry observations, and LOS accelerations measured from a 10 yr monitoring program of the 22 GHz maser emission of NGC 4258. The new model includes both disk warping and confocal elliptical maser orbits with differential precession. The distance to NGC 4258 is $7.60 \pm 0.17 \pm 0.15$ Mpc, a 3% uncertainty including formal fitting and systematic terms. The resulting Hubble constant, based on the use of the Cepheid variables in NGC 4258 to recalibrate the Cepheid distance scale, is $H_0 = 72.0 \pm 3.0$ km s^{-1} Mpc^{-1}.

Determining the Hubble constant H_0 using multiple calibrators

A 3% SOLUTION: DETERMINATION OF THE HUBBLE CONSTANT WITH THE *HUBBLE SPACE TELESCOPE* AND WIDE FIELD CAMERA 3*

Adam G. Riess et al. THE ASTROPHYSICAL JOURNAL, 730:119 (18pp), 2011 April 1

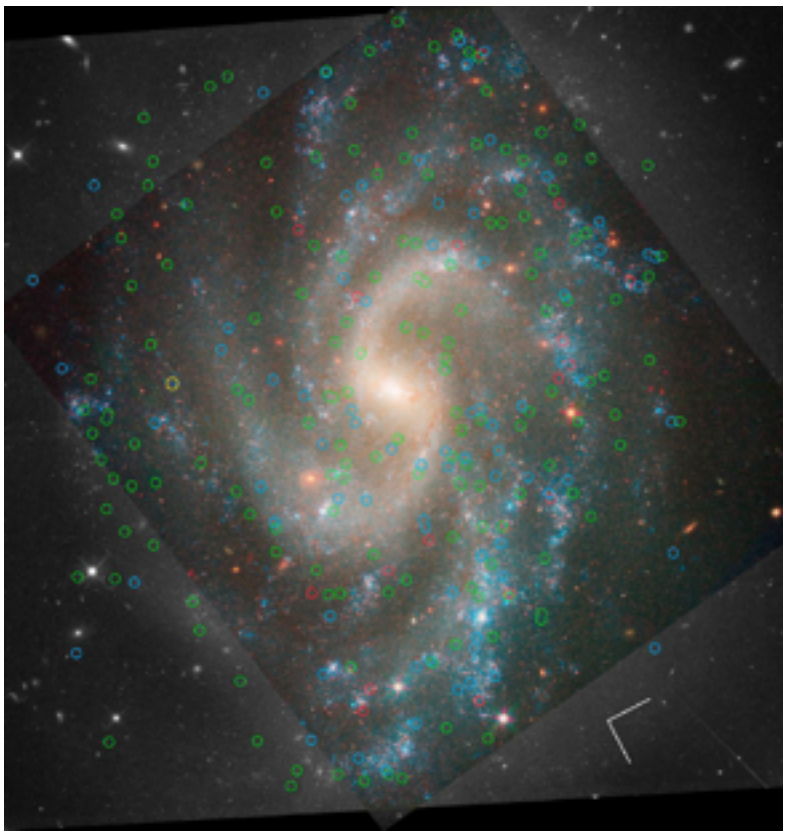

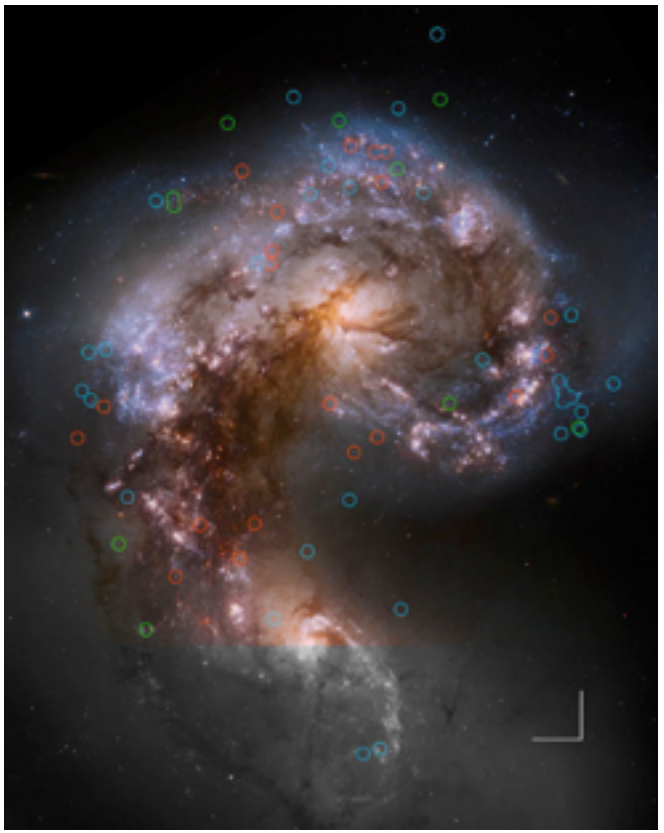

HST images of NGC 5584 and NGC 4038/9.. The positions of Cepheids with periods in the rangeP > 60 days, 30 days < P < 60 days, and 10 days < P < 30 days are indicated by red, blue, and green circles, respectively. A yellow circle indicates the position of the host galaxy's SN Ia. The orientation is indicated by the compass rose whose vectors have lengths of 15((and indicate north and east. The black and white regions of the images show the WFC3 optical data and the color includes the WFC3–IR data.

Determining the Hubble constant H_0 using multiple calibrators

A 3% SOLUTION: DETERMINATION OF THE HUBBLE CONSTANT WITH THE *HUBBLE SPACE TELESCOPE* AND WIDE FIELD CAMERA 3

Adam G. Riess et al. THE ASTROPHYSICAL JOURNAL, 730:119 (18pp), 2011 April 1

$H_0 = 73.8 \pm 2.4$ km s^{-1} Mpc^{-1} including systematic errors, corresponding to a 3.3% uncertainty.

Figure 9. Uncertainties in the determination of the Hubble constant. Uncertainties are squared to show their contribution to the quadrature sum. These terms are given in Table 5.

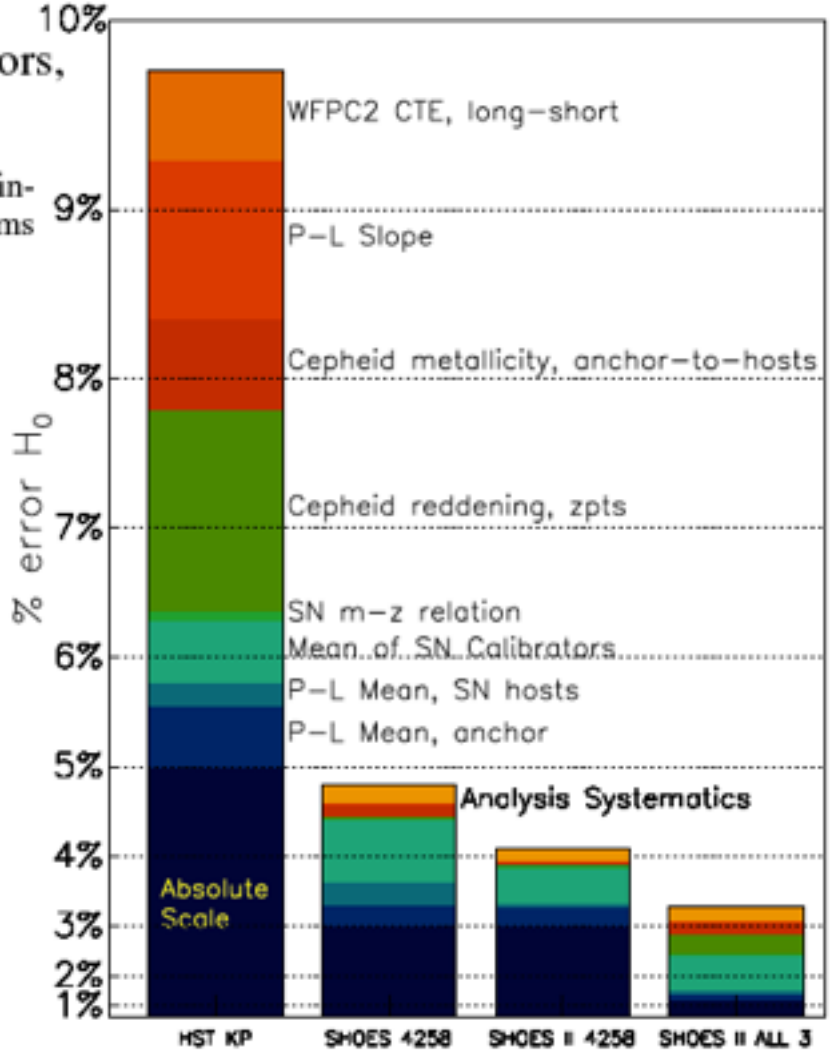

Table 5
H_0 Error Budget for Cepheid and SN Ia Distance Ladders[a]

Term	Description	Previous LMC	R09 N4258	Here N4258	Here All Three[b]
σ_{anchor}	Anchor distance	5%	3%	3%	1.3%
$\sigma_{anchor-PL}$	Mean of P–L in anchor	2.5%	1.5%	1.4%	0.7%[c]
$\sigma_{host-PL}/\sqrt{n}$	Mean of P–L values in SN hosts	1.5%	1.5%	0.6 %	0.6%
$\sigma_{SN}/\sqrt{n}$	Mean of SN Ia calibrators	2.5%	2.5%	1.9%	1.9%
σ_{m-z}	SN Ia m–z relation	1%	0.5%	0.5%	0.5%
$R\sigma_{\lambda,1,2}$	Cepheid reddening, zero points, anchor-to-hosts	4.5%	0.3%	0.0%	1.4%
σ_Z	Cepheid metallicity, anchor-to-hosts	3%	1.1%	0.6 %	1.0%
σ_{PL}	P–L slope, $\Delta\log P$, anchor-to-hosts	4%	0.5%	0.4%	0.6%
σ_{WFPC2}	WFPC2 CTE, long-short	3%	0%	0%	0%
Subtotal, σ_{H_0}		10%	4.7 %	4.0%	2.9%
Analysis systematics		NA	1.3%	1.0%	1.0%
Total, σ_{H_0}		10%	4.8 %	4.1%	3.1%

Notes.
[a] Derived from diagonal elements of the covariance matrix propagated via the error matrices associated with Equations (1), (3), (7), and (8).
[b] Using the combination of all three calibrations of the Cepheid distance scale, LMC, MW parallaxes, and NGC 4258.
[c] For MW parallax, this term is already included with the term above.

Monthly Notices of the ROYAL ASTRONOMICAL SOCIETY
MNRAS Advance Access published March 19, 2014

H_0 revisited

George Efstathiou
Kavli Institute for Cosmology and Institute of Astronomy, Madingley Road, Cambridge CB3 OHA, UK

ABSTRACT

I reanalyse the Riess et al. (hereafter R11) Cepheid data using the revised geometric maser distance to NGC 4258 of Humphreys et al. (hereafter H13). I explore different outlier rejection criteria designed to give a reduced χ^2 of unity and compare the results with the R11 rejection algorithm, which produces a reduced χ^2 that is substantially less than unity and, in some cases, leads to underestimates of the errors on parameters. I show that there are sub-luminous low-metallicity Cepheids in the R11 sample that skew the global fits of the period–luminosity relation. This has a small but non-negligible impact on the global fits using NGC 4258 as a distance scale anchor, but adds a poorly constrained source of systematic error when using the Large Magellanic Cloud as an anchor. I also show that the small Milky Way Cepheid sample with accurate parallax measurements leads to a distance to NGC 4258 that is in tension with the maser distance. I conclude that H_0 based on the NGC 4258 maser distance is $H_0 = 70.6 \pm 3.3\,\mathrm{km\,s^{-1}\,Mpc^{-1}}$, compatible within 1σ with the recent determination from *Planck* for the base six-parameter Λ cold dark matter cosmology. If the H-band period–luminosity relation is assumed to be independent of metallicity and the three distance anchors are combined, I find $H_0 = 72.5 \pm 2.5\,\mathrm{km\,s^{-1}\,Mpc^{-1}}$, which differs by 1.9σ from the *Planck* value. The differences between the *Planck* results and these estimates of H_0 are not large enough to provide compelling evidence for new physics at this stage.